# A Compact Wideband Millimeter-Wave Beam-Scanning Antenna Array for Industry 4.0 and Beyond Applications

Abdul Jabbar[1], Zhibo Pang[2], Ghazanfar Ali Safdar[3], Qammer Abbasi[1], Muhammad Ali Imran[1], Masood Ur-Rehman[1]
[1]James Watt School of Engineering, University of Glasgow, United Kingdom
[2]Automation Technology, ABB, Vasteras, Sweden
[3]Department of Computer Science & Technology, University of Bedfordshire, United Kingdom

***Abstract*—In this paper, a compact wideband series-fed 8-element linear antenna array is designed that covers the entire unlicensed 60 GHz band from 57–71 GHz. The linear 1 × 8 array has a simulated -10 dB impedance bandwidth of 35.21 % (50.53 to 72.13 GHz). The peak realized gain of 8-element array is 13.3 dBi at 60.5 GHz. The gain variation is less than 1 dB from 57–66 GHz and the overall gain is above 11.5 dBi up to 71 GHz. Side-lobe levels are below -10 dB in both E and H-planes, with low cross-polarization levels. The proposed array also manifests frequency-dependent beam-scanning in the elevation plane (y-z plane) from -10° to +35°. The proposed array is suitable for millimeter-wave industrial applications which require high bandwidth and multi-gigabits-per-second data rate. The designed array can work on various 60 GHz communication protocols such as IEEE 802.11ad, IEEE 802.11ay, IEEE 802.15.3c, Wireless HD and ECMA-387.**

***Keywords—60 GHz antenna array, beam-scanning, series fed array, IEEE 802.11ad/ay, millimeter-wave antenna.***

## I. INTRODUCTION

Industry 4.0 and Industry 5.0 are digital paradigms which demand high reliability, high throughput, and low latency. The digital drivers to envisage these industrial revolutions are the industrial Internet of Things (IIoT), digital twins, big data, 3D manufacturing, artificial intelligence, advanced wireless communication and smart sensor networks, to name but a few [1]. To enhance the efficiency of factory automation and smart manufacturing processes and to provide customized and personalized user experience, many sophisticated industrial applications come to play such as intelligent logistics, remote visual monitoring and surveillance, high precision image-guided automated assemblies, smart automatic robots and automatic guided vehicles, as well as image-based fault detection and product tracking, to list but a few [2], [3]. These applications require high bandwidth, throughput, reliability, and low latency [4]. However, traditional sub-6 GHz unlicensed bands such as 2.4 and 5 GHz are not able to fully meet such requirements due to some serious impediments such as limited bandwidth, interference and high spectral congestion. Therefore, the 60 GHz unlicensed industrial, scientific and medical (ISM) millimeter-wave (mmWave) band is envisaged as a potential enabler to meet the demands of next-generation industrial applications [3], [5].

The unlicensed 60 GHz band covers 57 to 66 GHz (9 GHz bandwidth) in most geographical areas of the world (Europe, Japan, Russia), whereas 57-71 GHz (14 GHz bandwidth) is being utilized in the USA and Canada under the ambit of 5G new radio (NR) and 3GPP latest releases [6]. For indoor industrial applications, IEEE 802.11ad and 802.11ay are key 60 GHz protocols [7], [8]. The 14 GHz bandwidth is divided into 6 channels with each channel having minimum bandwidth of 2.16 GHz. Therefore, from an antenna design perspective, a 60 GHz mmWave antenna must cover at least 2.16 GHz bandwidth to support at least one such channel [5]. Moreover, IEEE 802.11ay protocol supports channel bonding and channel aggregation, thus 4 such channels can be combined to achieve 8.64 GHz bandwidth with a single wide channel [7].

At 60 GHz band, path loss becomes a serious issue as it increases directly with the square of the operating frequency. Moreover, oxygen absorption of signals is high around 60 GHz which also results in loss of the received signal [9]. According to the Friis equation, with omnidirectional antennas at the transmitter and receiver side with 0 dBi gain each, and +10 dBm transmit power, the received power level becomes -58 dBm. However, the received power can be increased to -32 dBm (20 dB increase) using directional high-gain antennas with 13 dBi gain. Thus, to mitigate high path loss at 60 GHz, a high gain beamforming antenna array is crucial

Various antenna design techniques are employed at 60 GHz such as on-chip antennas [10], low-temperature co-fired ceramic (LTCC) based antennas [11] and printed circuit board (PCB) based antennas [12]–[19]. On-chip antennas suffer from low gain and low radiation efficiency due to the high permittivity and low resistivity of the silicon substrate. On the other hand, LTCC-based antennas are expensive and difficult to fabricate. Because of the high permittivity of LTTC materials, strong surface waves are produced which degrade antenna radiation patterns and increase cross-coupling [11]. However, PCB-based antennas are usually low cost, easy to fabricate and provide ease of integration with RF frontend circuitry.

In [14] and [15], a substrate-integrated waveguide (SIW) based 60 GHz antenna array is reported, which is complex to fabricate and the antenna size is quite large. Although a high-efficiency antenna was reported in [17], the achieved impedance bandwidth was up to 64 GHz with limited gain flatness and large size. In [18], a microstrip patch array was designed from 55 to 68 GHz, but the size and gain variation in the proposed band were high. Moreover, many of the other reported PCB-based antenna designs do not fully cover 14 GHz of worldwide unlicensed 60 GHz (from 57–71 GHz) with high gain flatness throughout the band. It is thus analyzed from the literature that a wideband 60 GHz antenna design covering all 6 channels (57–71 GHz) with high gain in the whole band of interest is demanded as well as challenging.

In this paper, a wideband microstrip patch series-fed array is designed to cover the entire 14 GHz of bandwidth (57–71 GHz). The proposed array consists of 8 linear elements series-fed configuration, while the array size is 13 mm × 25 mm × 0.2 mm.

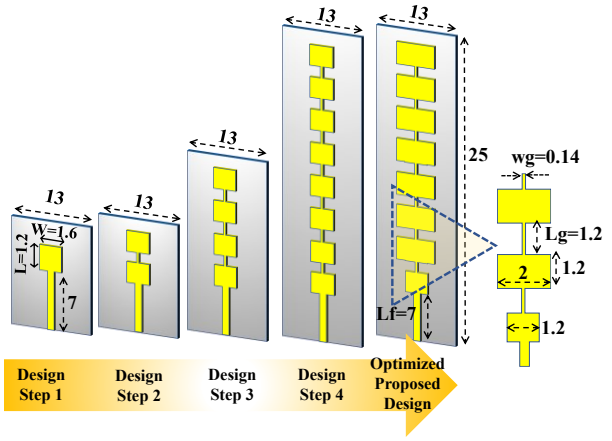


Fig. 1. Design evolution steps of proposed 1 × 8 linear series-fed array antenna (dimensions in millimeter).

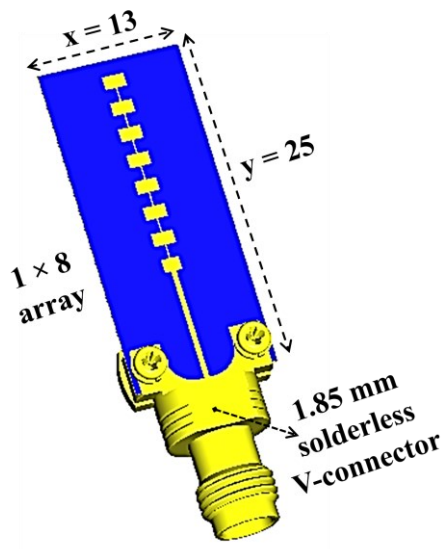


Fig. 2. Schematic model of the proposed 1 × 8 array with the model of V-connector co-simulated in CST (dimensions are in millimeter).

## II. Antenna Array Design

The proposed linear antenna array is based on microstrip patch elements. First, the width and length of a microstrip patch element were calculated using standard patch antenna equations at 60 GHz resonant frequency [20]. The width and length were set as 1.6 mm and 1.2 mm respectively as labelled in Fig. 1. A full ground plane was used at the bottom to achieve a broadside radiation pattern. The input impedance of the antenna was matched to 50 Ω using a feed line's width of 0.48 mm according to the substrate parameters.

Generally, patch antennas are inherently narrowband. In this work, the impedance bandwidth of the single patch element is not matched to resonate in the 60 GHz band because usually it also narrows down the overall -10 dB impedance bandwidth of the subsequent array. In contrast to conventional patch antenna impedance matching approaches, the proposed design does not include any inset slots. In order to enhance the matched impedance bandwidth, multiple resonances were purposefully introduced by using multiple series-fed elements with carefully optimized dimensions. As the RF signal travels in the series array, the loading impedance of each patch

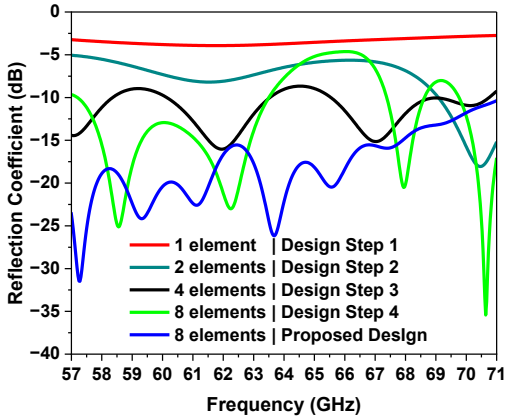


Fig. 3. Magnitude of reflection coefficient ($|S_{11}|$) for various antenna design evolution steps.

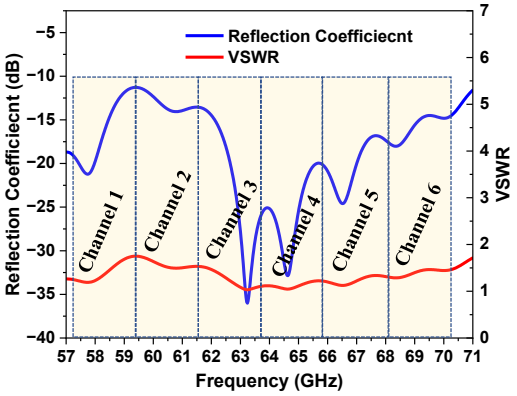


Fig. 4. Simulated reflection coefficient of the proposed 1 × 8 array.

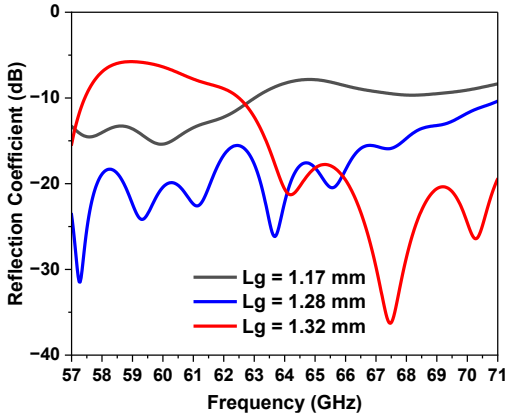


Fig. 5. Effect of interconnecting series-fed length (*Lg*) on the magnitude of the reflection coefficient for 1 × 8 array. The optimized length is 1.28 mm.

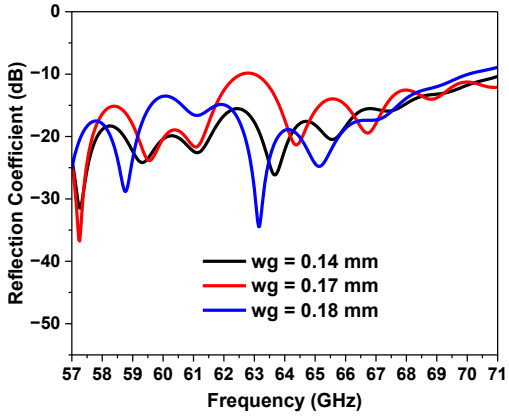


Fig. 6. Effect of change in width of series-fed transmission line (*wg*) on impedance bandwidth.

element changes (with varying phases), and different resonant modes appear in spectral proximity in a way that they get close to each other. As a result, a wideband -10 dB impedance matching was achieved. Such a design evolution to reach an 8-element series-fed array is shown in Fig. 1. As can be seen from Fig. 1, the first patch element of the 8-element array has a narrow width of 1.6 mm, while seven other patches have a relatively wider width (2 mm). Such type of tapering in the width improved -10 dB impedance bandwidth to cover the entire 57–71 GHz band.

The finalized optimum design of 8-element series-fed linear array is shown Fig. 2. The width of the full array was set at 13 mm because the footprint of the edge launch solderless V-connector (1.85 mm standard) is at least 12 mm. Therefore, since the beginning, realistic simulations were performed to analyze the connector effect. It is instructive to mention that the connector effect might be prominent at 60 GHz band, as its size becomes greater than the free space wavelength ($\lambda_o = 5$ mm at 60 GHz). However, it is noteworthy that in practice, the antenna is directly connected to RF frontend and the connector is not present.

The simulation results and array analysis are presented in the next section.

## III. Simulation Results and Array Analysis

The proposed antenna prototype is simulated using a low-loss Rogers 4003C substrate with a dielectric constant of 3.55, substrate thickness of 0.2 mm, a loss tangent of 0.002, and copper conductor thickness of 0.0175 mm. As shown in Fig. 1, initially identical patches were replicated where the effect of increasing the number of patch elements (2, 4, and 8) on impedance bandwidth (where $|S_{11}| < -10$ dB) was analyzed. The simulated reflection coefficients (|S11|) of various design evolution steps are shown in Fig. 3. As the number of elements was increased, multiple resonances occurred in the band of interest and wider impedance bandwidth was achieved. However, with the similar replicated 8-element array, the magnitude of the reflection coefficient was above -10 dB from 63.5 GHz to 67.5 GHz. To improve that, except for the first patch, the width of the other seven patches was optimized to 2mm (instead of 1.6 mm) for the proposed 1 × 8 array, as shown in Fig. 2. This provided an excellent -10 dB impedance bandwidth and the reflection coefficient of the proposed 1× 8 series-fed array is below -10 dB from 51.7–71.2 GHz, entirely covering 57-71 GHz band, as shown in Fig. 4.

The length of interconnecting series-feed transmission line (*Lg*) plays a significant role in achieving wide bandwidth. This is because the length of this transmission line directly affects the overall electrical length of patch antennas and thus the resonance frequency. The effect of variations in *Lg* is shown in Fig. 5. The width of the series-feed line (*wg*) however does not affect bandwidth significantly, as shown in Fig. 6. A better way is to optimize width to a minimum value according to practical fabrication limits.

To analyze the effect of the length of feed line (*Lf*), a parametric analysis of varying feed lengths is shown in Fig. 7, which reveals no significant effect on bandwidth (obviously within a range of careful dimensional limits). The long feed length of 7 mm is used to create a reasonable gap between the connector and the radiating patches so that the radiation pattern is not influenced by the connector during practical antenna measurements. Else, as mentioned

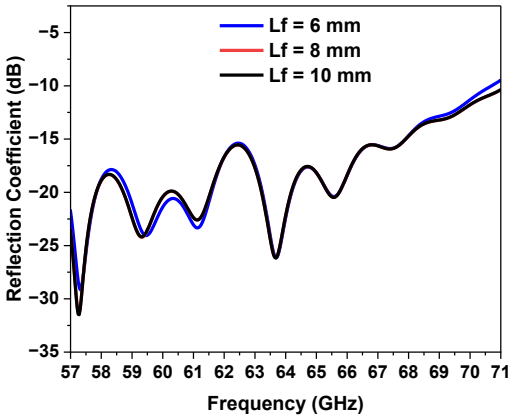


Fig. 7. Effect of variation in the length of feed line on the magnitude of the reflection coefficient.

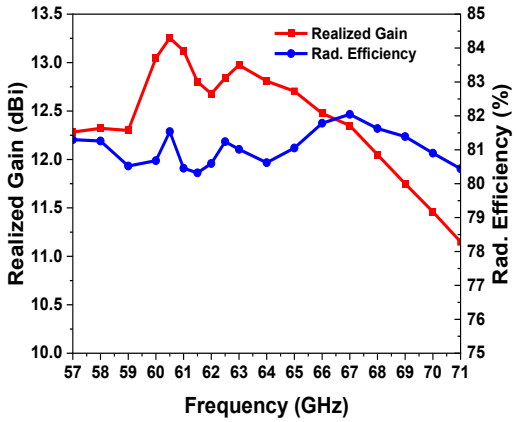


Fig. 8. Simulated realized gain and radiation efficiency of the proposed 1 × 8 array.

above, in practical RF circuits the antenna is directly connected to RF frontend and the connector is not present inside the circuitry.

The peak realized gain of the proposed 1 × 8 array is 13.25 dBi at 60.5 GHz. The realized gain is above 12.3 dBi from 57-66 GHz and above 11 dBi till 71 GHz, as shown in Fig.8, thus high gain flatness is achieved. The radiation efficiency is above 80% in the whole band of interest. The 3D realized gain patterns at different frequencies in the band of interest are shown in Fig. 8. It ca be noticed from Fi. 8 that the radiation pattern is stable across the whole band of interest.

As depicted in Fig. 8, a fan-shaped radiation pattern is observed with wider half-power beamwidth (HPBW) (70° to 130°) in x-z plane and low HPBW (12.1° to 14°) in y-z plane over the band. This is because the net radiation pattern is squeezed in the direction of array elements (the reason for low beamwidth in phi 90°) and spreads like a fan-shape in the plane perpendicular to the direction of the linear array (in phi 0°). The 2D heat map at 60.5 GHz in Fig. 9 also illustrates fan-shaped pattern with wider beamwidth around phi 0° and theta 0°–90° region, The front-to-back ratio is higher than 30 dB throughout the band of interest. Side-lobe levels (SLL) are well below -10 dB in both E and H-planes over the whole band as can be observed from Fig. 8. Excellent cross-polarization levels (less than -60 dB) are achieved in both E and H-planes.

As a future extension of this work, we aim to design a planar array using a corporate-feed network along with the

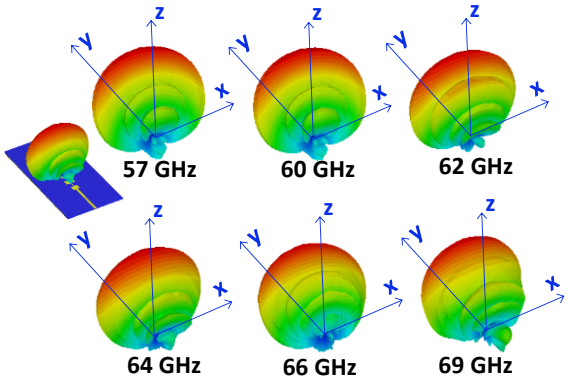


Fig. 8. 3D realized gain patterns at different frequencies in 60 GHz ISM band.

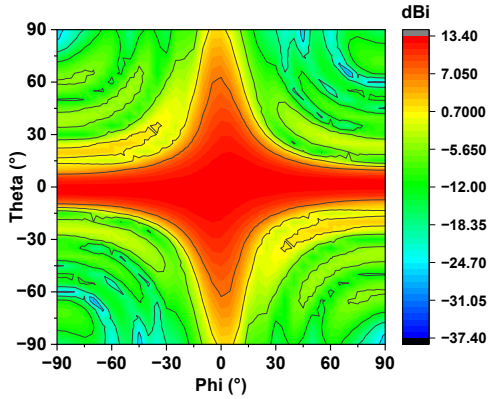


Fig. 9. 2D heta map at 60.5 GHz illustrating wideer beamwidth (fan-shaped) around phi 0°, and theta 0° to 90°.

proposed 1 × 8 linear array. Moreover, the proposed array can also be used to develop wideband multiple-input-multiple-output (MIMO) array configurations.

## IV. Conclusion

A compact, planar, and wideband mmWave microstrip antenna array is designed which covers the entire 57-71 GHz band (35.21% fractional bandwidth). The linear 8-element array achieved a peak gain of 13.3 dBi at 60.5 GHz. High gain flatness is achieved over 10 GHz of bandwidth from 57–67 GHz. The array design methodology and performance are thoroughly elucidated. The proposed antenna array works at various 60 GHz protocols such as IEEE 802.11ad. 802.11ay, 802.15.3c, ECMA-387 and WirelessHD.

## References

[1] E. Sisinni, A. Saifullah, S. Han, U. Jennehag, and M. Gidlund, "Industrial internet of things: Challenges, opportunities, and directions," *IEEE transactions on industrial informatics*, vol. 14, no. 11, pp. 4724–4734, 2018.

[2] Z. Pang, M. Luvisotto, and D. Dzung, "Wireless high-performance communications: The challenges and opportunities of a new target," *IEEE Industrial Electronics Magazine*, vol. 11, no. 3, pp. 20–25, 2017.

[3] M. Cheffena, "Industrial wireless communications over the millimeter wave spectrum: opportunities and challenges," *IEEE Communications Magazine*, vol. 54, no. 9, pp. 66–72, 2016.

[4] A. Jabbar, M. A. Jamshed, M. A. Shawky, Q. H. Abbasi, M. A. Imran, and M. Ur Rehman, "Multi-Gigabit Millimeter-Wave Industrial Communication: A Solution for Industry 4.0 and Beyond," *IEEE GLOBECOM*, 2022.

[5] A. Jabbar *et al.*, "Millimeter-Wave Smart Antenna Solutions for URLLC in Industry 4.0 and Beyond," *Sensors*, vol. 22, no. 7, p. 2688, 2022, doi: 10.3390/s22072688.

[6] S. Lagen *et al.*, "New radio beam-based access to unlicensed spectrum: Design challenges and solutions," *IEEE Communications Surveys \& Tutorials*, vol. 22, no. 1, pp. 8–37, 2019, doi: 10.1109/COMST.2019.2949145.

[7] P. Zhou *et al.*, "IEEE 802.11 ay-based mmWave WLANs: Design challenges and solutions," *IEEE Communications Surveys \& Tutorials*, vol. 20, no. 3, pp. 1654–1681, 2018.

[8] T. Nitsche, C. Cordeiro, A. B. Flores, E. W. Knightly, E. Perahia, and J. C. Widmer, "IEEE 802.11 ad: directional 60 GHz communication for multi-Gigabit-per-second Wi-Fi," *IEEE Communications Magazine*, vol. 52, no. 12, pp. 132–141, 2014.

[9] T. S. Rappaport, J. N. Murdock, and F. Gutierrez, "State of the art in 60-GHz integrated circuits and systems for wireless communications," *Proceedings of the IEEE*, vol. 99, no. 8, pp. 1390–1436, 2011, doi: 10.1109/JPROC.2011.2143650.

[10] H. M. Cheema and A. Shamim, "The last barrier: on-chip antennas," *IEEE Microwave Magazine*, vol. 14, no. 1, pp. 79–91, 2013.

[11] U. Ullah, N. Mahyuddin, Z. Arifin, M. Z. Abdullah, and A. Marzuki, "Antenna in LTCC technologies: a review and the current state of the art," *IEEE Antennas and Propagation Magazine*, vol. 57, no. 2, pp. 241–260, 2015.

[12] X.-P. Chen, K. Wu, L. Han, and F. He, "Low-cost high gain planar antenna array for 60-GHz band applications," *IEEE Transactions on Antennas and Propagation*, vol. 58, no. 6, pp. 2126–2129, 2010.

[13] H. Sun, Y.-X. Guo, and Z. Wang, "60-GHz circularly polarized U-slot patch antenna array on LTCC," *IEEE Transactions on Antennas and Propagation*, vol. 61, no. 1, pp. 430–435, 2012.

[14] A. Sarkar and S. Lim, "60 GHz compact larger beam scanning range PCB leaky-wave antenna using HMSIW for millimeter-wave applications," *IEEE Transactions on Antennas and Propagation*, vol. 68, no. 8, pp. 5816–5826, 2020.

[15] H. Chu, J.-X. Chen, and Y.-X. Guo, "An efficient gain enhancement approach for 60-GHz antenna using fully integrated vertical metallic walls in LTCC," *IEEE Transactions on Antennas and Propagation*, vol. 64, no. 10, pp. 4513–4518, 2016.

[16] B. Biglarbegian, M. Fakharzadeh, D. Busuioc, M.-R. R. Nezhad-Ahmadi, and S. Safavi-Naeini, "Optimized microstrip antenna arrays for emerging millimeter-wave wireless applications," *IEEE Transactions on antennas and propagation*, vol. 59, no. 5, pp. 1742–1747, 2011, doi: 10.1109/TAP.2011.2123058.

[17] Y. Al-Alem and A. A. Kishk, "Efficient millimeter-wave antenna based on the exploitation of microstrip line discontinuity radiation," *IEEE Transactions on Antennas and Propagation*, vol. 66, no. 6, pp. 2844–2852, 2018.

[18] W. Yang, K. Ma, K. S. Yeo, and W. M. Lim, "A compact high-performance patch antenna array for 60-GHz applications," *IEEE Antennas and Wireless Propagation Letters*, vol. 15, pp. 313–316, 2015, doi: 10.1109/LAWP.2015.2443054.

[19] A. S. W. Ghattas, A. A. R. Saad, and E. E. M. Khaled, "Compact patch antenna array for 60 GHz millimeter-wave broadband applications," *Wireless Personal Communications*, vol. 114, no. 4, pp. 2821–2839, 2020.

[20] C. A. Balanis, *Antenna theory: analysis and design*. John wiley \& sons, 2015.